A Fast Technique of Tissue Biomechanical Analysis for Real-time Prostate Tissue Elasticity Reconstruction

S. Reza Mousavi[a1] and Abbas Samani[a,b,c]

[a]Department of Electrical and Computer Engineering, The University of Western Ontario, London, ON, Canada;
[b]Department of Medical Biophysics, The University of Western Ontario, London, ON, Canada;
[c]Imaging Research Laboratories, Robarts Research Institute (RRI), London, ON, Canada

ABSTRACT

Elastography image reconstruction techniques typically involve displacement or stress field calculation of tissue undergoing mechanical stimulation that can be done by Finite Element (FE) analysis. However, traditional FE method is time-consuming, and hence not suitable for real-time or near real-time applications. In this article, we present an alternate accelerated method of stress calculation that can be incorporated in elastography reconstruction algorithms. Shape is an essential input of FE models that is considered in conjunction with material stiffness and loading to yield stress distribution. The essence of the proposed technique is finding a function between shape and stress field. This function takes the shape parameters as input and outputs the stress field very fast. To develop such a function principal component analysis (PCA) is used to obtain the main modes of shape and stress fields. As such, the shape and stress fields can be described by these main modes weighted by a small number of weight factors. Then, an efficient mapping technique is developed to relate the weight factors of shape to those of the stress fields. We used Neural Network (NN) for this mapping, which is the sought function required to input shape and output stress field. Once the mapping function is obtained it can be used for analyzing shapes not included in the NN training database. We employed this technique for prostate tissue stress analysis. For a typical prostate, our results indicate that analysis using our technique takes less than 0.07 seconds on a regular desktop computer irrespective of the model size and complexity. This analysis indicates that stress error of the majority of the samples is less than 5% per node.

Keywords: Prostate Cancer, Stress Analysis, Finite Element, Real-time, Principal Component Analysis

1 INTRODUCTION

Prostate cancer is the most common cancer in Canadian men. Prostate tumors usually grow slowly, and if detected early, it can often be cured or managed successfully [1]. For many years Digital Rectal Examination (DRE), Prostate-Specific Antigen (PSA) and Trans Rectal Ultra Sonography (TRUS) have been the primary techniques for prostate cancer detection [2]. However, these conventional methods have low sensitivity and specificity for prostate cancer detection [3]. For instance, comparison of TRUS-based diagnosis of prostate cancer to pathological evaluation (gold standard) found that ultrasound based diagnosis has a sensitivity of 52% and a specificity of 68% [4]. In contrast, it has been shown that there is a strong correlation between pathological and mechanical properties of soft tissue [5]. As such, based on the fact that variations in tissue elastic properties are associated with the presence of cancer [6], elastography in conjunction with US imaging can detect prostate cancer with a higher sensitivity [7].

Ultrasound elastography is a novel imaging technique in which elastic properties of tissues are reconstructed and displayed. Elastography image reconstruction techniques typically involve displacement or stress field calculation of tissue undergoing mechanical stimulation. This can be done by Finite Element Method (FEM), which is time-consuming, hence is not suitable for real-time or near real-time applications. In this work, we present an alternate accelerated method of tissue stress calculation that can be incorporated in real-time elastography reconstruction algorithms. This method develops a mapping scheme between shape space (e.g. different prostate shapes) and stress space. This mapping function can calculate the tissue stress field in real-time or near real-time fashion.

[1] Corresponding author. E-mail: smousav8@uwo.ca, Telephone: +1(226)374-4776.

(a) **(b)** **(c)**

Figure 1. 2D TRUS Images (a) before compression and (b) after compression. Points on the green line are free to move while points on the red lines are almost fixed. (c) Sample prostate-tumor model.

2 METHODOLOGY

2.1 Modeling

In order to calculate a displacement or stress field of tissue undergoing mechanical stimulation, FEM modeling can be used which requires the geometry and biomechanical properties of the tissue and boundary conditions. In this work, 2D TRUS images were used to construct the model. Based on these images (Fig. 1), mechanical stimulation is applied to the bottom of the prostate using ultrasound probe, which compresses the prostate and its surrounding tissue. The prostate tissue along with a block of surrounding tissue is incorporated in the model since the effect of the probe compression becomes insignificant at points far away from its application region. Hence, as shown in Fig. 1c, our model contains the prostate with a tumor inside a rectangular area mimicking the surrounding connective tissue. All points on the rectangle's edges are fixed except some points in the middle of the bottom edge where the probe applies compression. Different Young's moduli were assigned to the three regions of the tumor, prostate and surrounding tissue, and the model is discretized into a FE mesh. As the load acts in the plane of the 2D model (with small thickness) the problem is idealized as a plane stress problem.

2.2 FE Mapping Function

FEM is a time-consuming method; therefore, it is not suitable for real-time elasticity reconstruction. Tissue stress or displacement calculation can be accelerated if FEM is substituted by a mapping function that maps prostate shape into displacement and stress fields for a given loading. Establishing such a mapping function is possible because inter-patient prostate shape variability is modest while tissue deformation and stress distribution patterns under a given clinical mechanical stimulation are expected to be similar. Each prostate-tumour configuration can be represented by a set of points located on the boundary of the prostate and on the boundary of the tumour, called "landmarks". In order to compare equivalent points from different shapes, all shapes are aligned by scaling, rotation and translation with respect to a set of axes. Considering n landmarks, each shape in the shape space is given as follows:

$$X_i = \{x_{i,1}, y_{i,1}, x_{i,2}, y_{i,2}, ..., x_{i,n}, y_{i,n}\} \; i = 1, ..., N \tag{1}$$

where (x_i, y_i) are the coordinates of each landmark and N is the number of shapes in the shape space. As discussed earlier, each model should be meshed to be suitable for FE analysis. In this work, each shape was discritized using a common TFI-based FE mesh with quadrilateral elements [8], resulting in m elements for each shape. Conventional FE analysis provides accurate stresses at the elements' centroids [9]. Hence, different stress fields of each shape (e.g. σ_{yy}) obtained from FE analysis can be given as follows:

$$S_{yy,i} = \{S_{yy,i1}, S_{yy,i2}, ..., S_{yy,im}\} \; i = 1, ..., N \tag{2}$$

Because of the large array size of X and S, it is not efficient to establish a mapping function directly between vectors of 2n-D shape space and their corresponding vectors in m-D stress space. This may result in a complicated mapping function with a large number of parameters to be tuned. In order to have an efficient mapping, we find the main modes or principal components of both shape space and stress space, and then map the weight vectors of each space to their stress weight vectors counterparts.

2.2.1 Principal Component Analysis (PCA)

In PCA, main modes are specified by calculating the eigenvectors and eigenvalues of the covariance matrix of a space. Considering a space with N points, the covariance matrix of it is defined as:

$$Cov = \frac{1}{N-1}\sum_{i=1}^{N}(x_i - \bar{x})(x_i - \bar{x})^T, \quad \bar{x} = \frac{1}{N}\sum_{i=1}^{N} x_i \tag{3}$$

Eigenvectors of Cov are the orthogonal components of this space and their corresponding eigenvalues show how significant they are. The larger the eigenvalue the more significant is the corresponding eigenvector. Hence, based on the eigenvalues of the shape space, the L most significant eigenvectors $P = (p_1\ p_2 \ldots p_L)$ are adopted as the main modes of the shape space such that the ratio of the sum of the corresponding L eigenvalues to the sum of all eigenvalues is more than 0.99. Similarly, the T most significant eigenvectors of the stress space $Q = (q_1\ q_2 \ldots q_T)$ are adopted as the main modes of that space. According to PCA, the vectors of each space are mapped to its main modes resulting in vectors of weight factors:

$$\begin{aligned} X_i &= \bar{X} + b_i P \ \Rightarrow\ b_i = P^{+}(X_i - \bar{X}) \\ S_i &= \bar{S} + c_i Q \ \Rightarrow\ c_i = Q^{+}(S_i - \bar{S}) \end{aligned} \tag{4}$$

In which P^{+} and Q^{+} are the pseudo-inverse matrices of P and Q, respectively.

Stress field of tissue undergoing mechanical stimulation depends on both shape and Young's modulus distribution. Therefore, the Young's moduli of tissues are added to the weight factors of points in the shape space and the mapping function is established between the resulting augmented vectors ($[b_i\ E_i]$) and vectors of weight factors in the stress space (c_i).

2.2.2 Mapping Function Computation

We use Neural Networks (NN) to relate shapes and stress fields. The NN we used for this purpose is a multi-layer feed-forward back propagation neural network. In general, Multilayer Feed Forward Neural Network (FFNN) [10] is widely used in function approximation applications. Such networks consist of an input layer, which conducts the inputs to the next layer, a number of hidden layers and an output layer. Hidden and output layers include a number of neurons. Each neuron receives a number of weighted inputs as well as a bias and yields an output. To compute its output, each neuron uses a transfer function over the sum of its weighted inputs and bias. During the training phase, the network finds an optimum mapping relationship between the input and output vectors using training samples, i.e. a number of input vectors and their corresponding known output vectors. This is carried out by the network through adjusting its neurons' weights and bias values to minimize the differences between the network's known responses to their respective input samples. The most common training algorithm used in FFNN is the back-propagation algorithm, which is based on the gradient descent method. The term back-propagation refers to the manner in which the gradient is computed for nonlinear multilayer networks. In the simulation phase, the trained network responds to new input vectors based on its knowledge achieved during the training phase to produce the output. In this study, a three-layer feed-forward back-propagation neural network was applied for function approximation. The NN's topology was chosen such that the input layer has the size of input vector $[b_i\ E_i]$ with one hidden layer consisting of 15 neurons in addition to the output layer. The output layer includes as many neurons as the size of c_i. All the neurons used 'tansig' as their transfer function except the output neurons that used 'purelin' as transfer function.

3 RESULTS

A database of 1000 prostate-tumour configurations was produced to evaluate the proposed method. The fitting NN was trained with 800 out of the 1000 samples. 200 additional samples were then used to test the mapping function. Results were validated by FE analysis results obtained by ABAQUS (commercial FEM software). Figure 2 shows the average error per node for 200 test samples. Figure 2 indicates that the majority of the samples have errors of less than 5% while only very few samples encounter errors larger than 10%. The latter ones are the ones that correspond to very small stress values, hence their percentage error is amplified. Stress fields resulting from conventional FE analysis and from FFNN function for a typical test sample are depicted in Fig.3. This figure shows a very good agreement between these fields. Figure 4 shows the difference of the two result sets. It indicates that the difference in regions near the contact nodes and boundaries of prostate and tumor is higher than other regions.

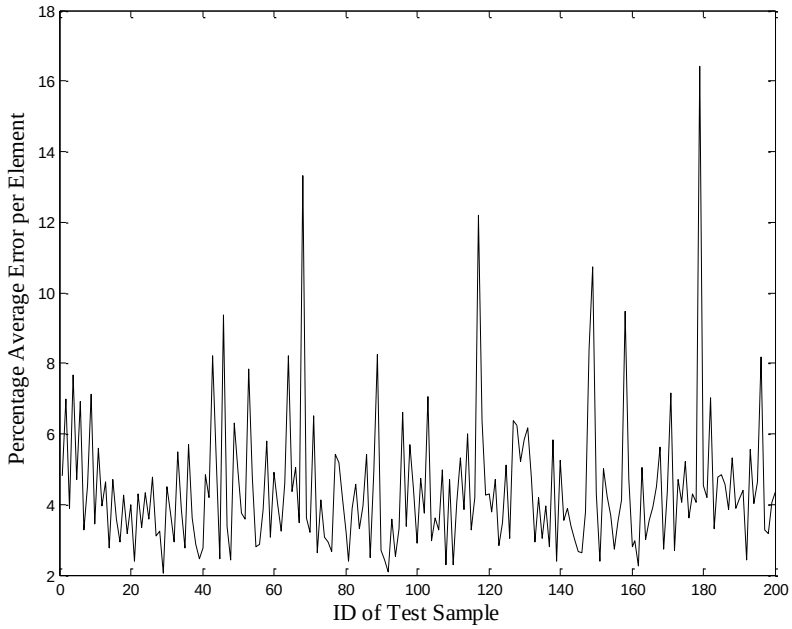

Figure 2. Percentage average error per element of stress field for 200 test samples (using 800 training samples).

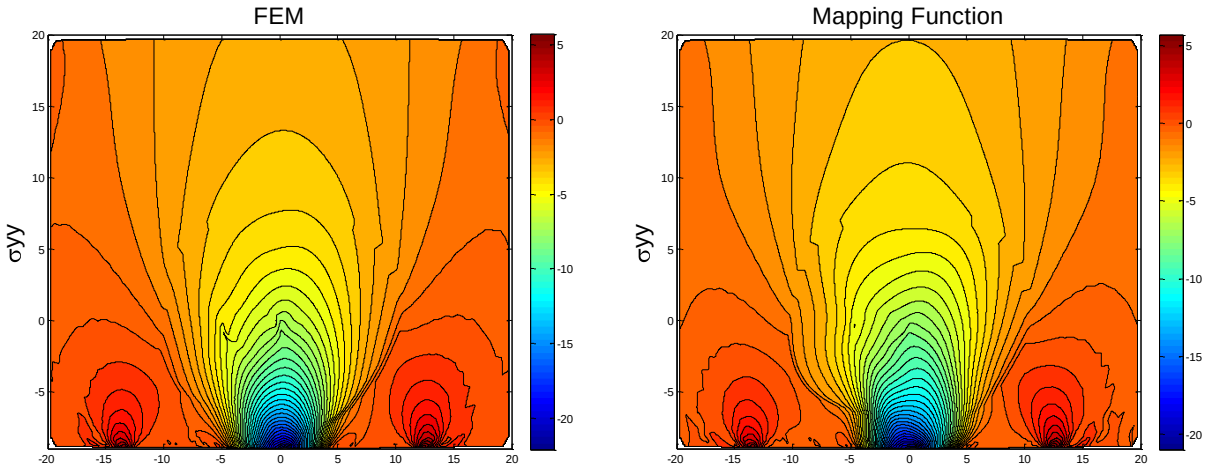

Figure 3. Stress field resulted from (a) FEM and (b) FFNN mapping function.

4 CONCLUSION AND DISCUSSION

In this paper, we presented a fast method for estimating stress field of tissue under specified loading conditions. The proposed method establishes a mapping function to relate shape space and stress space. Due to the large number of variables required to define the shape and stress spaces, PCA was employed to reduce the dimensions by projecting both the shape and stress spaces to their main modes. The resulting compact spaces were then interrelated via a neural network model. The proposed method is both fast and accurate for calculating stress field of the same class of objects. Further work is under way to use this mapping for our new real-time elastography modulus reconstruction technique in which prostate and tumor moduli are updated iteratively using strain images acquired from an ultrasound imaging system and stress field estimated with the proposed method.

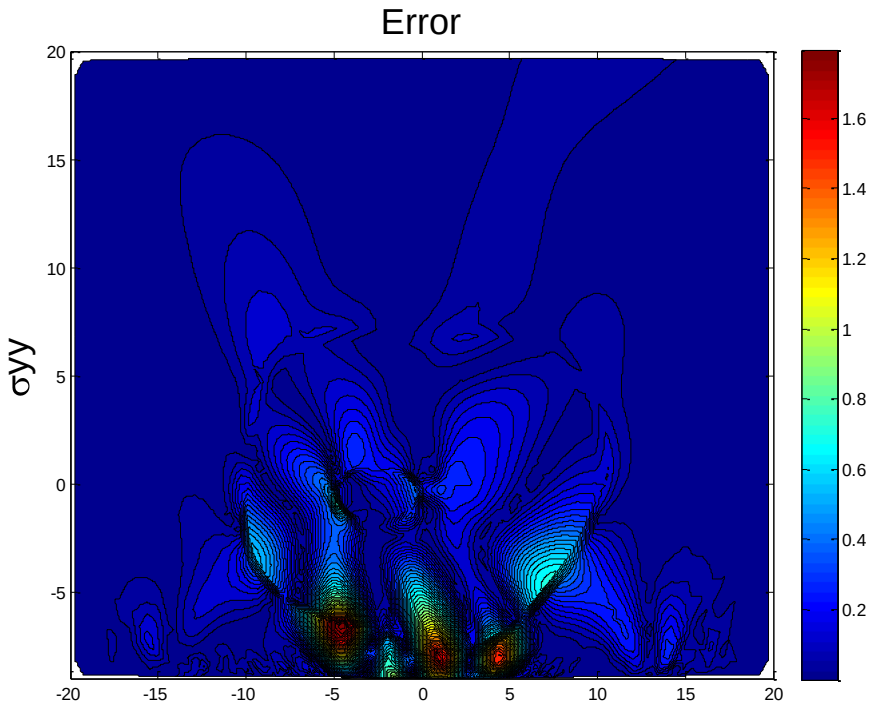

Figure 4. Difference of Stress fields resulting from FEM and FFNN mapping function.

References

[1] Canadian Cancer society: www.cancer.ca.

[2] K. Kamoi, K. Okihara, A. Ochiai, O. Ukimura, Y. mizutani, A. Kawauchi, and T. Miki, 'The Utility of Transrectal Real-Time Elastography in the Diagnosis of Prostate Cancer," *Ultrasound in Med. & Biol.* **34**, pp. 1025–1032, 2008.

[3] G. Salomon, J. Kollerman, I. Thederan, F. K.H. Chun, L. Budaus, T. Schlomm, H. Isbarn, H. Heinzer, H. Huland, and M. Graefen, "Evaluation of Prostate Cancer Detection with Ultrasound Real-Time Elastography: A Comparison with Step Section Pathological Analysis after Radical Prostatectomy," *European Urology* **54**, pp. 1354–1362, 2008.

[4] H. B. Carter, U. M. Hamper, and S. Sheth, "Evaluation of Transrectal Ultrasound in the Early Detection of Prostate Cancer," *J. of Urol.* **142**, pp. 1008-101, 1989.

[5] T. A. Krouskop, T. M. Wheeler, F. Kallel, B. S. Garra, and T. Hall, "Elastic Moduli of Breast and Prostate Tissues under Compression," *J. of Ultrasound Imaging* **20,** pp. 260-274, 1998.

[6] A. Samani, J. Bishop, and D. B. Plewes, "A Constrained Modulus Reconstruction Technique for Breast Cancer Assessment," *IEEE Trans. Medical Imaging* **20**, 2001.

[7] K. Konig, U. Scheipers, A. Pesavento, A. Lorenz, H. Ermert, and T. Senge, "Initial Experiences with Real-Time Elastography Guided Biopsies of the Prostate." *J. of Urol.* **174**, pp. 115-117, 2005.

[8] P. M. Knupp, S. Steinberg, *Fundamentals of Grid Generation*, CRC Press, 1994.

[9] *ABAQUS/Standard User's Manual*, Habbit, Kalson & Sorensen, Inc., Version 6.3, 2002.

[10] N. Toda, K. I. Funahashi, S. Usui, "Polynomial functions can be realized by finite size multilayer feedforward neural networks," *Proc. IEEE Int. Joint Conf. Neural Networks*, pp. 343-384, Singapore. 1991.